

Search for Scalar Top Quark Production in $p\bar{p}$ Collisions at $\sqrt{s} = 1.8$ TeV

T. Affolder,²¹ H. Akimoto,⁴³ A. Akopian,³⁶ M. G. Albrow,¹⁰ P. Amaral,⁷ S. R. Amendolia,³²
D. Amidei,²⁴ K. Anikeev,²² J. Antos,¹ G. Apollinari,³⁶ T. Arisawa,⁴³ T. Asakawa,⁴¹
W. Ashmanskas,⁷ M. Atac,¹⁰ F. Azfar,²⁹ P. Azzi-Bacchetta,³⁰ N. Bacchetta,³⁰ M. W. Bailey,²⁶
S. Bailey,¹⁴ P. de Barbaro,³⁵ A. Barbaro-Galtieri,²¹ V. E. Barnes,³⁴ B. A. Barnett,¹⁷
M. Barone,¹² G. Bauer,²² F. Bedeschi,³² S. Belforte,⁴⁰ G. Bellettini,³² J. Bellinger,⁴⁴
D. Benjamin,⁹ J. Bensinger,⁴ A. Beretvas,¹⁰ J. P. Berge,¹⁰ J. Berryhill,⁷ S. Bertolucci,¹²
B. Bevensee,³¹ A. Bhatti,³⁶ C. Bigongiari,³² M. Binkley,¹⁰ D. Bisello,³⁰ R. E. Blair,²
C. Blocker,⁴ K. Bloom,²⁴ B. Blumenfeld,¹⁷ S. R. Blusk,³⁵ A. Bocci,³² A. Bodek,³⁵
W. Bokhari,³¹ G. Bolla,³⁴ Y. Bonushkin,⁵ D. Bortoletto,³⁴ J. Boudreau,³³ A. Brandl,²⁶
S. van den Brink,¹⁷ C. Bromberg,²⁵ M. Brozovic,⁹ N. Bruner,²⁶ E. Buckley-Geer,¹⁰
J. Budagov,⁸ H. S. Budd,³⁵ K. Burkett,¹⁴ G. Busetto,³⁰ A. Byon-Wagner,¹⁰ K. L. Byrum,²
M. Campbell,²⁴ A. Caner,³² W. Carithers,²¹ J. Carlson,²⁴ D. Carlsmith,⁴⁴ J. Cassada,³⁵
A. Castro,³⁰ D. Cauz,⁴⁰ A. Cerri,³² A. W. Chan,¹ P. S. Chang,¹ P. T. Chang,¹ J. Chapman,²⁴
C. Chen,³¹ Y. C. Chen,¹ M. -T. Cheng,¹ M. Chertok,³⁸ G. Chiarelli,³² I. Chirikov-
Zorin,⁸ G. Chlachidze,⁸ F. Chlebana,¹⁰ L. Christofek,¹⁶ M. L. Chu,¹ S. Cihangir,¹⁰
C. I. Ciobanu,²⁷ A. G. Clark,¹³ M. Cobal,³² E. Cocca,³² A. Connolly,²¹ J. Conway,³⁷
J. Cooper,¹⁰ M. Cordelli,¹² D. Costanzo,³² J. Cranshaw,³⁹ D. Cronin-Hennessy,⁹ R. Cropp,²³
R. Culbertson,⁷ D. Dagenhart,⁴² F. DeJongh,¹⁰ S. Dell'Agnello,¹² M. Dell'Orso,³²
R. Demina,¹⁰ L. Demortier,³⁶ M. Deninno,³ P. F. Derwent,¹⁰ T. Devlin,³⁷ J. R. Dittmann,¹⁰
S. Donati,³² J. Done,³⁸ T. Dorigo,¹⁴ N. Eddy,¹⁶ K. Einsweiler,²¹ J. E. Elias,¹⁰ E. Engels,
Jr.,³³ W. Erdmann,¹⁰ D. Errede,¹⁶ S. Errede,¹⁶ Q. Fan,³⁵ R. G. Feild,⁴⁵ C. Ferretti,³²
I. Fiori,³ B. Flaughier,¹⁰ G. W. Foster,¹⁰ M. Franklin,¹⁴ J. Freeman,¹⁰ J. Friedman,²²
Y. Fukui,²⁰ S. Galeotti,³² M. Gallinaro,³⁶ T. Gao,³¹ M. Garcia-Sciveres,²¹ A. F. Garfinkel,³⁴
P. Gatti,³⁰ C. Gay,⁴⁵ S. Geer,¹⁰ D. W. Gerdes,²⁴ P. Giannetti,³² P. Giromini,¹² V. Glagolev,⁸
M. Gold,²⁶ J. Goldstein,¹⁰ A. Gordon,¹⁴ A. T. Goshaw,⁹ Y. Gotra,³³ K. Goulianatos,³⁶
H. Grassmann,⁴⁰ C. Green,³⁴ L. Groer,³⁷ C. Grossi-Pilcher,⁷ M. Guenther,³⁴ G. Guillian,²⁴
J. Guimaraes da Costa,²⁴ R. S. Guo,¹ C. Haber,²¹ E. Hafen,²² S. R. Hahn,¹⁰ C. Hall,¹⁴
T. Handa,¹⁵ R. Handler,⁴⁴ W. Hao,³⁹ F. Happacher,¹² K. Hara,⁴¹ A. D. Hardman,³⁴
R. M. Harris,¹⁰ F. Hartmann,¹⁸ K. Hatakeyama,³⁶ J. Hauser,⁵ J. Heinrich,³¹ A. Heiss,¹⁸
M. Herndon,¹⁷ B. Hinrichsen,²³ K. D. Hoffman,³⁴ C. Holck,³¹ R. Hollebeek,³¹ L. Holloway,¹⁶
R. Hughes,²⁷ J. Huston,²⁵ J. Huth,¹⁴ H. Ikeda,⁴¹ M. Incagli,³² J. Incandela,¹⁰ G. Introzzi,³²
J. Iwai,⁴³ Y. Iwata,¹⁵ E. James,²⁴ H. Jensen,¹⁰ M. Jones,³¹ U. Joshi,¹⁰ H. Kambara,¹³
T. Kamon,³⁸ T. Kaneko,⁴¹ K. Karr,⁴² H. Kasha,⁴⁵ Y. Kato,²⁸ T. A. Keaffaber,³⁴ K. Kelley,²²
M. Kelly,²⁴ R. D. Kennedy,¹⁰ R. Kephart,¹⁰ D. Khazins,⁹ T. Kikuchi,⁴¹ M. Kirk,⁴
B. J. Kim,¹⁹ H. S. Kim,¹⁶ M. J. Kim,¹⁹ S. H. Kim,⁴¹ Y. K. Kim,²¹ L. Kirsch,⁴
S. Klimenko,¹¹ P. Koehn,²⁷ A. Konigeter,¹⁸ K. Kondo,⁴³ J. Konigsberg,¹¹ K. Kordas,²³
A. Korn,²² A. Korytov,¹¹ E. Kovacs,² J. Kroll,³¹ M. Kruse,³⁵ S. E. Kuhlmann,² K. Kurino,¹⁵
T. Kuwabara,⁴¹ A. T. Laasanen,³⁴ N. Lai,⁷ S. Lami,³⁶ S. Lammel,¹⁰ J. I. Lamoureux,⁴
M. Lancaster,²¹ G. Latino,³² T. LeCompte,² A. M. Lee IV,⁹ S. Leone,³² J. D. Lewis,¹⁰
M. Lindgren,⁵ T. M. Liss,¹⁶ J. B. Liu,³⁵ Y. C. Liu,¹ N. Lockyer,³¹ J. Loken,²⁹ M. Loreti,³⁰
D. Lucchesi,³⁰ P. Lukens,¹⁰ S. Lusin,⁴⁴ L. Lyons,²⁹ J. Lys,²¹ R. Madrak,¹⁴ K. Maeshima,¹⁰
P. Maksimovic,¹⁴ L. Malferrari,³ M. Mangano,³² M. Mariotti,³⁰ G. Martignon,³⁰ A. Martin,⁴⁵

J. A. J. Matthews,²⁶ P. Mazzanti,³ K. S. McFarland,³⁵ P. McIntyre,³⁸ E. McKigney,³¹ M. Menguzzato,³⁰ A. Menzione,³² E. Meschi,³² C. Mesropian,³⁶ T. Miao,¹⁰ R. Miller,²⁵ J. S. Miller,²⁴ H. Minato,⁴¹ S. Miscetti,¹² M. Mishina,²⁰ N. Moggi,³² E. Moore,²⁶ R. Moore,²⁴ Y. Morita,²⁰ A. Mukherjee,¹⁰ T. Muller,¹⁸ A. Munar,³² P. Murat,³² S. Murgia,²⁵ M. Musy,⁴⁰ J. Nachtman,⁵ S. Nahn,⁴⁵ H. Nakada,⁴¹ T. Nakaya,⁷ I. Nakano,¹⁵ C. Nelson,¹⁰ D. Neuberger,¹⁸ C. Newman-Holmes,¹⁰ C.-Y. P. Ngan,²² P. Nicolaidi,⁴⁰ H. Niu,⁴ L. Nodulman,² A. Nomerotski,¹¹ S. H. Oh,⁹ T. Ohmoto,¹⁵ T. Ohsugi,¹⁵ R. Oishi,⁴¹ T. Okusawa,²⁸ J. Olsen,⁴⁴ C. Pagliarone,³² F. Palmonari,³² R. Paoletti,³² V. Papadimitriou,³⁹ S. P. Pappas,⁴⁵ D. Partos,⁴ J. Patrick,¹⁰ G. Paulette,⁴⁰ M. Paulini,²¹ C. Paus,²² L. Pescara,³⁰ T. J. Phillips,⁹ G. Piacentino,³² K. T. Pitts,¹⁰ R. Plunkett,¹⁰ A. Pompos,³⁴ L. Pondrom,⁴⁴ G. Pope,³³ M. Popovic,²³ F. Prokoshin,⁸ J. Proudfoot,² F. Ptohos,¹² G. Punzi,³² K. Ragan,²³ A. Rakitine,²² D. Reher,²¹ A. Reichold,²⁹ W. Riegler,¹⁴ A. Ribon,³⁰ F. Rimondi,³ L. Ristori,³² W. J. Robertson,⁹ A. Robinson,²³ T. Rodrigo,⁶ S. Rolli,⁴² L. Rosenson,²² R. Roser,¹⁰ R. Rossin,³⁰ W. K. Sakumoto,³⁵ D. Saltzberg,⁵ A. Sansoni,¹² L. Santi,⁴⁰ H. Sato,⁴¹ P. Savard,²³ P. Schlabach,¹⁰ E. E. Schmidt,¹⁰ M. P. Schmidt,⁴⁵ M. Schmitt,¹⁴ L. Scodellaro,³⁰ A. Scott,⁵ A. Scribano,³² S. Segler,¹⁰ S. Seidel,²⁶ Y. Seiya,⁴¹ A. Semenov,⁸ F. Semeria,³ T. Shah,²² M. D. Shapiro,²¹ P. F. Shepard,³³ T. Shibayama,⁴¹ M. Shimojima,⁴¹ M. Shochet,⁷ J. Siegrist,²¹ G. Signorelli,³² A. Sill,³⁹ P. Sinervo,²³ P. Singh,¹⁶ A. J. Slaughter,⁴⁵ K. Sliwa,⁴² C. Smith,¹⁷ F. D. Snider,¹⁰ A. Solodsky,³⁶ J. Spalding,¹⁰ T. Speer,¹³ P. Sphicas,²² F. Spinella,³² M. Spiropulu,¹⁴ L. Spiegel,¹⁰ L. Stanco,³⁰ J. Steele,⁴⁴ A. Stefanini,³² J. Strologas,¹⁶ F. Strumia,¹³ D. Stuart,¹⁰ K. Sumorok,²² T. Suzuki,⁴¹ R. Takashima,¹⁵ K. Takikawa,⁴¹ M. Tanaka,⁴¹ T. Takano,²⁸ B. Tannenbaum,⁵ W. Taylor,²³ M. Tecchio,²⁴ P. K. Teng,¹ K. Terashi,⁴¹ S. Tether,²² D. Theriot,¹⁰ R. Thurman-Keup,² P. Tipton,³⁵ S. Tkaczyk,¹⁰ K. Tollefson,³⁵ A. Tollestrup,¹⁰ H. Toyoda,²⁸ W. Trischuk,²³ J. F. de Troconiz,¹⁴ J. Tseng,²² N. Turini,³² F. Ukegawa,⁴¹ J. Valls,³⁷ S. Vejcik III,¹⁰ G. Velev,³² R. Vidal,¹⁰ R. Vilar,⁶ I. Volobouev,²¹ D. Vucinic,²² R. G. Wagner,² R. L. Wagner,¹⁰ J. Wahl,⁷ N. B. Wallace,³⁷ A. M. Walsh,³⁷ C. Wang,⁹ C. H. Wang,¹ M. J. Wang,¹ T. Watanabe,⁴¹ D. Waters,²⁹ T. Watts,³⁷ R. Webb,³⁸ H. Wenzel,¹⁸ W. C. Wester III,¹⁰ A. B. Wicklund,² E. Wicklund,¹⁰ H. H. Williams,³¹ P. Wilson,¹⁰ B. L. Winer,²⁷ D. Winn,²⁴ S. Wolbers,¹⁰ D. Wolinski,²⁴ J. Wolinski,²⁵ S. Wolinski,²⁴ S. Worm,²⁶ X. Wu,¹³ J. Wyss,³² A. Yagil,¹⁰ W. Yao,²¹ G. P. Yeh,¹⁰ P. Yeh,¹ J. Yoh,¹⁰ C. Yosef,²⁵ T. Yoshida,²⁸ I. Yu,¹⁹ S. Yu,³¹ A. Zanetti,⁴⁰ F. Zetti,²¹ and S. Zucchelli³

(CDF Collaboration)

¹ Institute of Physics, Academia Sinica, Taipei, Taiwan 11529, Republic of China

² Argonne National Laboratory, Argonne, Illinois 60439

³ Istituto Nazionale di Fisica Nucleare, University of Bologna, I-40127 Bologna, Italy

⁴ Brandeis University, Waltham, Massachusetts 02254

⁵ University of California at Los Angeles, Los Angeles, California 90024

⁶ Instituto de Fisica de Cantabria, University of Cantabria, 39005 Santander, Spain

⁷ Enrico Fermi Institute, University of Chicago, Chicago, Illinois 60637

⁸ Joint Institute for Nuclear Research, RU-141980 Dubna, Russia

⁹ Duke University, Durham, North Carolina 27708

¹⁰ Fermi National Accelerator Laboratory, Batavia, Illinois 60510

- 11 *University of Florida, Gainesville, Florida 32611*
- 12 *Laboratori Nazionali di Frascati, Istituto Nazionale di Fisica Nucleare, I-00044 Frascati, Italy*
- 13 *University of Geneva, CH-1211 Geneva 4, Switzerland*
- 14 *Harvard University, Cambridge, Massachusetts 02138*
- 15 *Hiroshima University, Higashi-Hiroshima 724, Japan*
- 16 *University of Illinois, Urbana, Illinois 61801*
- 17 *The Johns Hopkins University, Baltimore, Maryland 21218*
- 18 *Institut für Experimentelle Kernphysik, Universität Karlsruhe, 76128 Karlsruhe, Germany*
- 19 *Korean Hadron Collider Laboratory: Kyungpook National University, Taegu 702-701; Seoul National University, Seoul 151-742; and SungKyunKwan University, Suwon 440-746; Korea*
- 20 *High Energy Accelerator Research Organization (KEK), Tsukuba, Ibaraki 305, Japan*
- 21 *Ernest Orlando Lawrence Berkeley National Laboratory, Berkeley, California 94720*
- 22 *Massachusetts Institute of Technology, Cambridge, Massachusetts 02139*
- 23 *Institute of Particle Physics: McGill University, Montreal H3A 2T8; and University of Toronto, Toronto M5S 1A7; Canada*
- 24 *University of Michigan, Ann Arbor, Michigan 48109*
- 25 *Michigan State University, East Lansing, Michigan 48824*
- 26 *University of New Mexico, Albuquerque, New Mexico 87131*
- 27 *The Ohio State University, Columbus, Ohio 43210*
- 28 *Osaka City University, Osaka 588, Japan*
- 29 *University of Oxford, Oxford OX1 3RH, United Kingdom*
- 30 *Università di Padova, Istituto Nazionale di Fisica Nucleare, Sezione di Padova, I-35131 Padova, Italy*
- 31 *University of Pennsylvania, Philadelphia, Pennsylvania 19104*
- 32 *Istituto Nazionale di Fisica Nucleare, University and Scuola Normale Superiore of Pisa, I-56100 Pisa, Italy*
- 33 *University of Pittsburgh, Pittsburgh, Pennsylvania 15260*
- 34 *Purdue University, West Lafayette, Indiana 47907*
- 35 *University of Rochester, Rochester, New York 14627*
- 36 *Rockefeller University, New York, New York 10021*
- 37 *Rutgers University, Piscataway, New Jersey 08855*
- 38 *Texas A&M University, College Station, Texas 77843*
- 39 *Texas Tech University, Lubbock, Texas 79409*
- 40 *Istituto Nazionale di Fisica Nucleare, University of Trieste/ Udine, Italy*
- 41 *University of Tsukuba, Tsukuba, Ibaraki 305, Japan*
- 42 *Tufts University, Medford, Massachusetts 02155*
- 43 *Waseda University, Tokyo 169, Japan*
- 44 *University of Wisconsin, Madison, Wisconsin 53706*
- 45 *Yale University, New Haven, Connecticut 06520*

November 13, 1999

(submitted to Phys. Rev. Lett.)

Abstract

We have searched for direct production of scalar top quarks at the Collider Detector at Fermilab in 88 pb^{-1} of $p\bar{p}$ collisions at $\sqrt{s}=1.8 \text{ TeV}$. We assume the scalar top quark decays into either a bottom quark and a chargino or a bottom quark, a lepton, and a scalar neutrino. The event signature for both decay scenarios is a lepton, missing transverse energy, and at least two b -quark jets. For a chargino mass of $90 \text{ GeV}/c^2$ and scalar neutrino masses of at least $40 \text{ GeV}/c^2$, we find no evidence for scalar top production and present upper limits on the production cross section in both decay scenarios.

The Minimal Supersymmetric extension to the Standard Model (MSSM) [1] assigns a scalar supersymmetric partner for every Standard Model fermion and a fermionic superpartner for every Standard Model boson. The weak eigenstates of each scalar superpartner mix, forming mass eigenstates [2]. The splitting of the mass eigenvalues is proportional to the mass of the Standard Model partner. Therefore, the superpartners of the top quark weak eigenstates, \tilde{t}_L and \tilde{t}_R , may have the largest mass splitting of all the scalar quarks (squarks). The running of the squark mass parameters is proportional to the Yukawa coupling of the Standard Model partners, such that the diagonal elements of the \tilde{t}_L, \tilde{t}_R mass matrix should be smaller than those of the other squarks [2]. Thus, the lighter scalar top mass eigenstate, \tilde{t}_1 , is the best candidate for the lightest squark and is potentially lighter than the top quark. We report the results of a search for direct production of $\tilde{t}_1\bar{\tilde{t}}_1$ in $88\pm4\text{ pb}^{-1}$ of data collected during the 1994-95 Tevatron run using the Collider Detector at Fermilab (CDF).

The CDF detector has been described elsewhere [3]. In this analysis, we used electrons identified in the central electromagnetic calorimeter which covers the pseudorapidity region $|\eta| < 1.1$. We used muons identified by tracks in drift chambers in two detector subcomponents outside the calorimeters. The first muon subsystem is located behind five absorption lengths of material and covers the region $|\eta| < 0.6$. The second is located behind an additional three absorption lengths of material and has the same η coverage as the first.

Scalar tops are strongly produced in the Tevatron via $q\bar{q}$ annihilation and gluon-gluon fusion. We searched for $\tilde{t}_1\bar{\tilde{t}}_1$ production within the framework of the MSSM for the case where $m_{\tilde{t}_1} < m_t$. We assumed R-parity [2] is conserved and restricted ourselves to two separate \tilde{t}_1 decay modes [4]. In the first, the decay¹ $\tilde{t}_1 \rightarrow b\tilde{\chi}_1^+$, where $\tilde{\chi}_1^+$ is the lightest chargino, proceeds with a branching ratio of 100%. We required one of the charginos, which decay via a virtual W , to decay as $\tilde{\chi}_1^+ \rightarrow e^+\nu$ or $\mu^+\nu$, where $\tilde{\chi}_1^0$ is the lightest neutralino, with an assumed branching ratio of 11% for each lepton type. For models where $\tilde{t}_1 \rightarrow b\tilde{\chi}_1^+$ is not kinematically allowed, we considered a second decay scenario in which $\tilde{t}_1 \rightarrow bl^+\tilde{\nu}$, where $\tilde{\nu}$ is a scalar neutrino and each $l = e, \mu, \tau$ has a branching ratio of 33.3%. In these two scenarios, either the $\tilde{\chi}_1^0$ or the $\tilde{\nu}$ is the lightest supersymmetric particle (LSP) and does not decay. A third possible decay scenario in which the $\tilde{t}_1 \rightarrow c\tilde{\chi}_1^0$ branching ratio is 100% is the subject of separate CDF searches [5].

In both decay scenarios considered here, the \tilde{t}_1 signature is at least one isolated lepton, missing transverse energy (\cancel{E}_T) from the neutral LSP's and at least two jets from the b quarks. This signature is very similar to that of the top quark, with kinematic differences due to the smaller \tilde{t}_1 mass in our search region, the presence of two massive neutralinos in the final state, and the absence of a real W in the final state. We therefore expect events with lower lepton p_T , lower jet E_T and multiplicity, and without a peak in the lepton- \cancel{E}_T transverse mass. To remain efficient for the smaller \tilde{t}_1 mass, we used data collected with the low- p_T electron and muon triggers described in Ref. [6]. These trigger thresholds were $E_T \geq 8\text{ GeV}$ for electrons and $p_T \geq 8\text{ GeV}/c$ for muons.

The data for this analysis were obtained by requiring (i) an electron with $E_T \geq 10\text{ GeV}$ or muon with $p_T \geq 10\text{ GeV}/c$ originating from the primary vertex and passing lepton identification cuts, (ii) $\cancel{E}_T \geq 25\text{ GeV}$, and (iii) at least two jets with cone sizes of

¹Unless otherwise noted, decay channels imply their charge conjugates.

$R \equiv \sqrt{(\Delta\eta)^2 + (\Delta\phi)^2} = 0.7$, one with $E_T \geq 12$ GeV and the second with $E_T \geq 8$ GeV. The lepton identification cuts were identical to those used in previous CDF analyses [7,8]. For electron identification, the electron was required to have lateral and longitudinal shower profiles consistent with those of an electron, have less than 5% of its energy deposited in the hadronic calorimeter, and be well-matched to a track from the CTC. A muon was required to have tracks in the inner and outer central muon chambers which were well-matched to a track from the CTC. We further required the leptons to pass an isolation cut in which the calorimeter E_T in a cone of $R = 0.4$ around the lepton was less than 2 GeV (excluding the lepton tower). No explicit tau identification was conducted, but leptons from tau decays were accepted.

We used the SVX' detector to identify secondary vertices from b quark decays and selected events with at least one secondary vertex. The tagging algorithm is described in Ref. [7] with improvements given in Ref. [9] and efficiency measured in Ref. [10]. We reduced the Drell-Yan background in our sample by removing events with two isolated, opposite-sign leptons. This background was further reduced by removing events with an isolated lepton that reconstructed an invariant mass ≥ 50 GeV/c 2 with any additional, isolated CTC track. Finally, we reduced the background from $b\bar{b}$ events and events with hadrons misidentified as leptons (fake leptons) by requiring that the $\Delta\phi$ between the \cancel{E}_T and the nearer of the two highest- E_T jets be ≥ 0.5 rad. This reduces fake \cancel{E}_T due to jet energy mismeasurement. The number of events remaining in our sample after all cuts is 81.

Signal and background selection cut efficiencies were estimated using a variety of Monte Carlo generators followed by a CDF detector simulation. Signal event samples were created using ISAJET version 7.20 [11]. The supersymmetric particle masses used in signal simulation were: $m_{\tilde{\chi}_1^\pm} = 90$ GeV/c 2 , $m_{\tilde{\chi}_1^0} = 40$ GeV/c 2 , and $m_{\tilde{\nu}} \geq 40$ GeV/c 2 , which are consistent with current lower limits [12]. The signal selection efficiency increases with $m_{\tilde{t}_1}$ but decreases with $m_{\tilde{\nu}}$ and $m_{\tilde{\chi}_1^\pm}$, reaching a plateau as event energies advance from cut thresholds. Some specific efficiencies are 5.4% for $\tilde{t}_1 \rightarrow bl^+\tilde{\nu}$ ($m_{\tilde{t}_1} = 130$ GeV/c 2 , $m_{\tilde{\nu}} = 40$ GeV/c 2) and 0.7% for $\tilde{t}_1 \rightarrow b\tilde{\chi}_1^+$ ($m_{\tilde{t}_1} = 120$ GeV/c 2 , $m_{\tilde{\chi}_1^\pm} = 90$ GeV/c 2 , and $m_{\tilde{\chi}_1^0} = 40$ GeV/c 2). These selection efficiencies include branching ratios of forced decays.

The significant sources of uncertainty for signal selection efficiency are (i) the b -jet tagging efficiency, (ii) the trigger efficiencies, (iii) the luminosity, and (iv) initial- and final-state radiation. The effects of some of these sources vary with $m_{\tilde{t}_1}$, but none contribute more than 10% to the overall uncertainty, which is less than 16% for all $m_{\tilde{t}_1}$ considered.

Standard Model backgrounds come from any process that can produce two or more jets, either real or fake leptons, and real or fake \cancel{E}_T . This includes heavy flavor quark production, vector boson production with two or more accompanying jets, and inclusive jet production with real or fake leptons. The number of events from the first two processes that we expected in our data sample were predicted using measured or calculated cross sections and selection efficiencies determined from Monte Carlo. Top-pair and single-top production were simulated using HERWIG version 5.6 [13]. For $m_t = 175$ GeV/c 2 $\sigma_{t\bar{t}}$ is 5.1 ± 1.6 pb [10] and $\sigma_{t\bar{b}}$ for W -gluon fusion from a next-to-leading-order (NLO) calculation is 1.70 ± 0.15 pb [14]. Vector boson samples were generated using VECBOS version 3.03 [15] and normalized according to CDF measurement [16]. Drell-Yan, $b\bar{b}$, and $c\bar{c}$ samples were generated with ISAJET version 7.06 and normalized to independent CDF data samples.

To determine the number of events with fake leptons in our sample, we used a data

sample passing all our selection cuts with the exceptions of a non-overlapping \cancel{E}_T requirement ($15 \leq \cancel{E}_T \leq 20$ GeV) and no requirement on $\Delta\phi(\cancel{E}_T, \text{nearer jet})$. The number of fake lepton events was normalized to this data sample, which contained negligible signal, after other backgrounds were subtracted. The number of fake lepton events was then extrapolated to the signal region using cut efficiencies determined from an independent fake-lepton event sample.

The complete list of backgrounds and the number of expected events remaining after all cuts is given in Table I. The significant backgrounds are $t\bar{t}$, $b\bar{b}$, $W^\pm(\rightarrow l^\pm\nu) + \geq 2$ jets, and fake lepton events. The number of data events agrees well with the expected background.

To determine the number of potential signal events in this final data sample, we performed extended, unbinned likelihood fits for each \tilde{t}_1 mass considered for both decay scenarios. The likelihood fits compared the shapes of distributions of the signal and background and included Gaussian terms tying the fit background levels to their predicted levels. The fit parameters were the numbers of signal events, $t\bar{t}$ events, $b\bar{b}$ plus fake lepton events, and vector boson events (represented in the fit by the $W^\pm + \geq 2$ jets distributions). We used the Kolmogorov statistic applied to the simulated distributions of signal and combined backgrounds to determine the most sensitive kinematic distributions to use in the fit. The kinematic distributions evaluated include lepton p_T , H_T (the scalar sum of lepton E_T , \cancel{E}_T , and jet E_T for all jets with $E_T \geq 8$ GeV), jet multiplicity, and $\Delta\phi(\text{jet1}, \text{jet2})$, where jets are ordered in E_T .

For the $\tilde{t}_1 \rightarrow b\tilde{\chi}_1^+$ decay, sensitivity to signal was greatest for a two-dimensional fit to the combined probability distributions for H_T and $\Delta\phi(\text{jet1}, \text{jet2})$. Fit results at all masses were consistent with zero signal events. The fit result for $\tilde{t}_1 \rightarrow b\tilde{\chi}_1^+$ with $m_{\tilde{t}_1} = 115$ GeV/c², $m_{\tilde{\chi}_1^\pm} = 90$ GeV/c², and $m_{\tilde{\chi}_1^0} = 40$ GeV/c² is shown in Fig. 1. The 95% C.L. limits on $\sigma_{\tilde{t}_1\bar{t}_1}$ for this decay are shown in Fig. 2 as a function of $m_{\tilde{t}_1}$ [17]. The NLO prediction for $\sigma_{\tilde{t}_1\bar{t}_1}$ using the renormalization scale $\mu = m_{\tilde{t}_1}$ and parton distribution function CTEQ3M is shown in Fig. 2 for comparison [18].

For the $\tilde{t}_1 \rightarrow bl^+\tilde{\nu}$ decay scenario, sensitivity to signal was greatest for a fit to the H_T distribution. Again, all fit results were consistent with zero signal events. The 95% C.L. limits on $\sigma_{\tilde{t}_1\bar{t}_1}$ for the $\tilde{t}_1 \rightarrow bl^+\tilde{\nu}$ decay are shown in Fig. 3 for $m_{\tilde{\nu}} = 40$ and 50 GeV/c². We consider the regions of supersymmetric parameter space for which the 95% C.L. limit on $\sigma_{\tilde{t}_1\bar{t}_1}$ is less than the NLO prediction ($\mu = m_{\tilde{t}_1}$) to be excluded. The resulting excluded region in the plane of $m_{\tilde{t}_1}$ versus $m_{\tilde{\nu}}$ is shown in Fig. 4.

To conclude, we have searched for direct $\tilde{t}_1\bar{t}_1$ production in 88 ± 4 pb⁻¹ of data collected using the CDF detector during the 1994-95 Tevatron run. We found no evidence for $\tilde{t}_1\bar{t}_1$ production for either $\tilde{t}_1 \rightarrow b\tilde{\chi}_1^+$ or $\tilde{t}_1 \rightarrow bl^+\tilde{\nu}$ and present upper limits on $\sigma_{\tilde{t}_1\bar{t}_1}$ as a function of $m_{\tilde{t}_1}$.

We thank the Fermilab staff and the technical staffs of the participating institutions for their vital contributions. This work was supported by the U.S. Department of Energy and National Science Foundation; the Italian Istituto Nazionale di Fisica Nucleare; the Ministry of Education, Science and Culture of Japan; the National Sciences and Engineering Research Council of Canada; the National Science Council of the Republic of China; the A. P. Sloan Foundation; and the Swiss National Science Foundation.

REFERENCES

- [1] H. P. Nilles, Phys. Rep. **110**, 1 (1984); H. E. Haber and G. L. Kane, Phys. Rep. **117**, 75 (1985); M. F. Sohnius, Phys. Rep. **128**, 39 (1985); K. Cahill, *Elements of Supersymmetry*, hep-ph/9907295, (1999).
- [2] H. Baer *et al.*, Phys. Rev. D **44**, 725 (1991); S. Martin, *A Supersymmetry Primer*, hep-ph/9709356 (1997).
- [3] CDF Collaboration, F. Abe *et al.*, Nucl. Instr. and Meth. **A350**, 74 (1994), CDF Collaboration, F. Abe *et al.*, Phys. Rev. **D50**, 2966 (1994), and D. Amidei *et al.*, Nucl. Instr. and Meth. **A71** (1988).
- [4] K. Hikasa and M. Kobayashi, Phys. Rev. D **36**, 724 (1987).
- [5] CDF Collaboration, F. Abe *et al.*, *Search for Scalar Top and Scalar Bottom Quarks in $p\bar{p}$ Collisions at $\sqrt{s} = 1.8$ TeV*, submitted to Phys. Rev. Lett. ; F. Abe *et al.*, *Search for R parity violating supersymmetry using like sign dielectrons in $p\bar{p}$ collisions at $\sqrt{s} = 1.8$ TeV*, accepted by Phys. Rev. Lett.
- [6] CDF Collaboration, F. Abe *et al.*, Phys. Rev. D **58**, 092002 (1998).
- [7] CDF Collaboration, F. Abe *et al.*, Phys. Rev. D **50**, 2966 (1994).
- [8] CDF Collaboration, F. Abe *et al.*, Phys. Rev. Lett. **76**, 4307 (1996).
- [9] CDF Collaboration, F. Abe *et al.*, Phys. Rev. Lett. **74**, 2626 (1995).
- [10] F. Ptakos (for the CDF Collaboration), proceedings of the International Europhysics Conference on High Energy Physics 99, Tampere, Finland, July 17, 1999.
- [11] H. Baer, F.E. Paige, S.D. Protopopescu, and X. Tata, in *Simulating Supersymmetry with ISAJET 7.0/ISASUSY 1.0*, Proceedings of Workshop on Physics at Current Accelerators and the Supercollider, Eds. J. Hewett, A. White, and D. Zeppenfeld (Argonne National Laboratory, 1993).
- [12] F. Abe *et al.*, (The CDF Collaboration), Phys. Rev. Lett. **80**, 5275 (1998); R. Barate, *et al.*, (ALEPH Collaboration), Eur. Phys. J. C 2, 417 (1998); K. Ackerstaff, *et al.*, (OPAL Collaboration), Eur. Phys. J. C 2, 213 (1998).
- [13] G. Marchesini *et al.*, Comput. Phys. Commun. **67**, 465 (1992).
- [14] T. Stelzer, Z. Sullivan, and S. Willenbrock, Phys. Rev. D **56**, 5619 (1998).
- [15] F. A. Berends *et al.*, Nucl. Phys. **B357**, 32 (1991).
- [16] CDF Collaboration, F. Abe *et al.*, Phys. Rev. Lett. **79**, 4760 (1997).
- [17] To determine an upper limit when the mean is approaching zero, we use the method in G. Feldman and R. Cousins, Phys. Rev. D **57**, 3873 (1998).
- [18] W. Beenakker *et al.*, Nucl. Phys. **B515**, 3 (1998).
- [19] The LEP1 lower limits on $m_{\tilde{\nu}}$: ALEPH Collaboration, D. Decamp *et al.*, Phys. Rep. **216**, 253 (1992); DELPHI Collaboration, P. Abreu *et al.*, Nucl. Phys. **B367**, 511 (1991); L3 Collaboration, O. Adriani *et al.*, Phys. Rep. **236**, 1 (1993). LEP2 results for the $m_{\tilde{t}_1} - m_{\tilde{\nu}}$ exclusion plane are found in ALEPH Collaboration, R. Barate *et al.*, *Searches for Sleptons and Squarks in $e+e-$ Collisions at $\sqrt{s}=188.6$ GeV*, to be submitted to Phys. Lett. **B**.

TABLES

TABLE I. Number of data events and expected background events after all selection cuts. The dominant sources of uncertainty on the numbers of expected events are integrated luminosity, cross section, trigger efficiency, and b-jet tagging. (Fake leptons are hadron tracks which have been misidentified as leptons.)

process	number of events expected after all cuts
$W^\pm(\rightarrow e^\pm\nu \text{ or } \mu^\pm\nu) + \geq 2 \text{ jets}$	44.5 ± 7.3
$t\bar{t}$	17.8 ± 4.5
$b\bar{b}$	5.8 ± 0.8
$W^\pm(\rightarrow \tau^\pm\nu) + \geq 2 \text{ jets}$	2.6 ± 0.4
$t\bar{b}$ (from $W - g$ fusion)	1.6 ± 0.2
$Z(\rightarrow e^+e^- \text{ or } \mu^+\mu^-) + \geq 2 \text{ jets}$	1.4 ± 0.2
$Z(\rightarrow \tau^+\tau^-) + \geq 1 \text{ jet}$	0.4 ± 0.1
$\gamma \rightarrow l^+l^-$	0.4 ± 0.1
$c\bar{c}$	0.06 ± 0.02
fake lepton events	12.7 ± 1.6
background total	87.3 ± 8.8
data	81

FIGURES

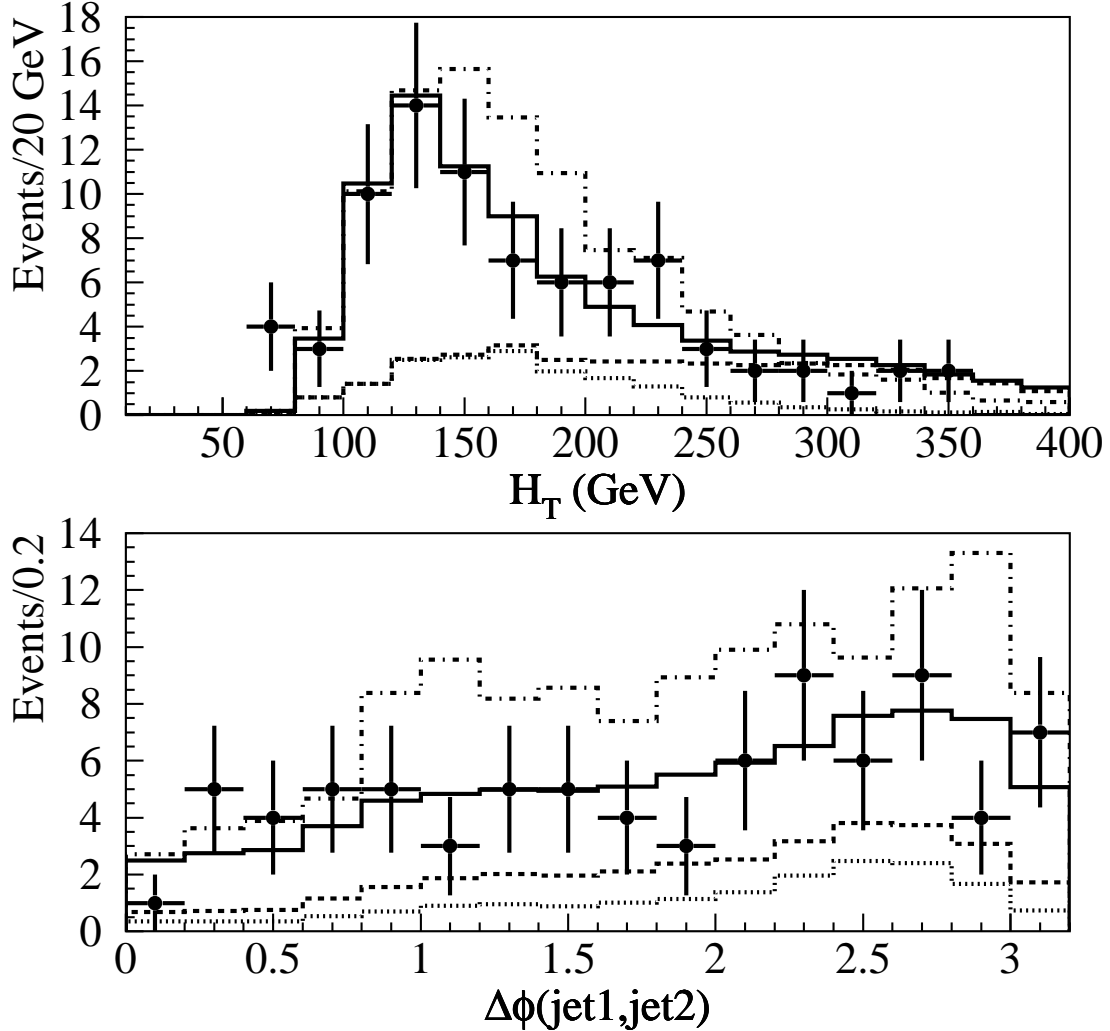


FIG. 1. Results of the two-dimensional fit to H_T and $\Delta\phi(\text{jet1}, \text{jet2})$ when the $\tilde{t}_1 \rightarrow b\tilde{\chi}_1^+$ branching ratio is 100%, $m_{\tilde{t}_1} = 115 \text{ GeV}/c^2$, $m_{\tilde{\chi}_1^\pm} = 90 \text{ GeV}/c^2$, and $m_{\tilde{\chi}_1^0} = 40 \text{ GeV}/c^2$. The quantities H_T and $\Delta\phi(\text{jet1}, \text{jet2})$ are defined in the text. The points represent the data. Cumulative contributions from $b\bar{b}$ and fake lepton events, $t\bar{t}$, and $W^\pm \rightarrow l^\pm\nu + \text{jets}$ are represented by dotted, dashed and solid lines respectively. There is no significant contribution from signal. To illustrate the shape difference, a signal distribution with arbitrary normalization has been overlaid with a dot-dash line.

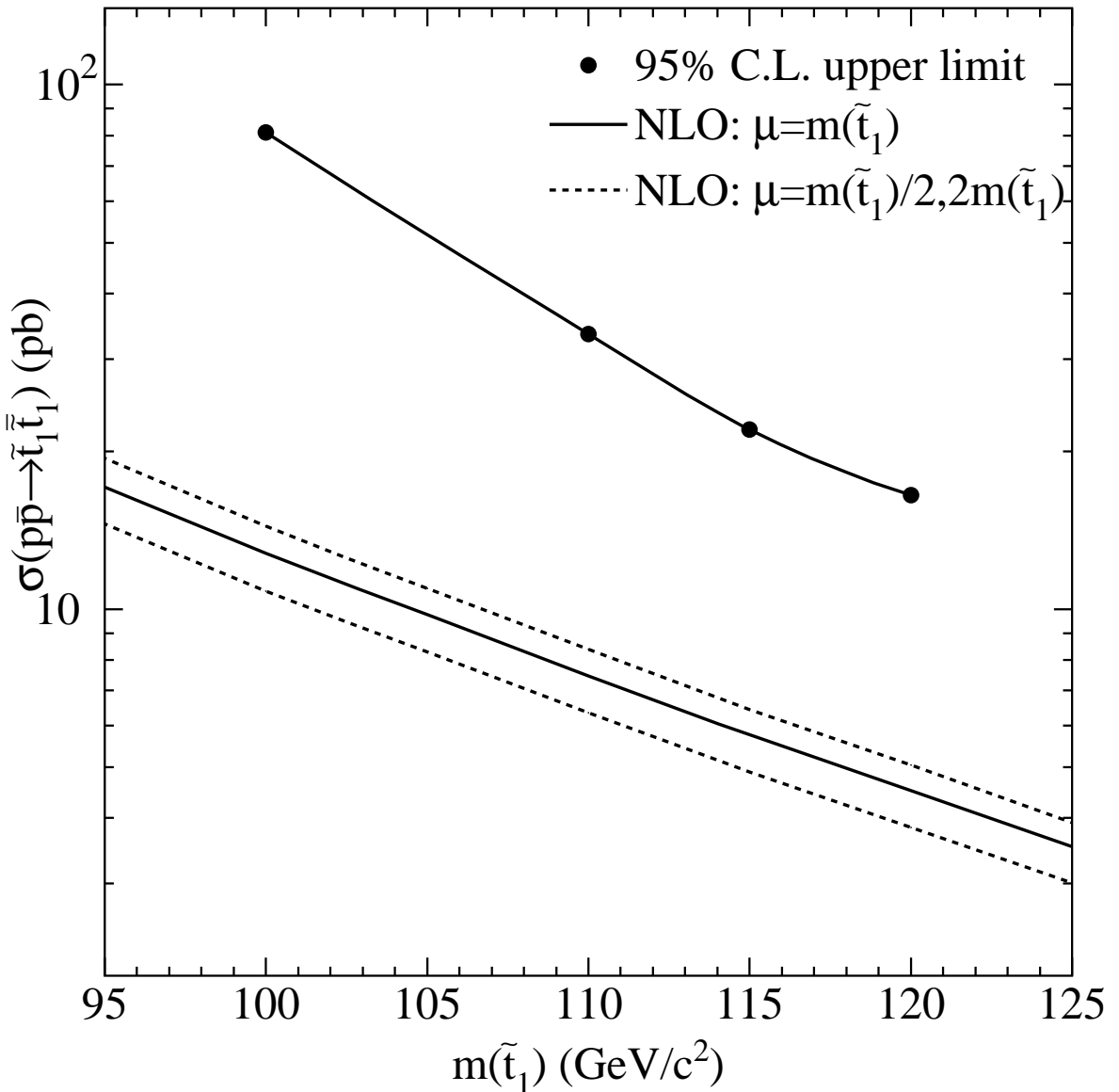


FIG. 2. The points represent the CDF 95% C.L. cross section limit as a function of \tilde{t}_1 mass when the $\tilde{t}_1 \rightarrow b\tilde{\chi}_1^+$ branching ratio is 100%, $m_{\tilde{\chi}_1^\pm} = 90$ GeV/c², and $m_{\tilde{\chi}_1^0} = 40$ GeV/c². The line without markers represents the NLO prediction for $\sigma_{\tilde{t}_1 \bar{\tilde{t}}_1}$ using the renormalization scale $\mu = m_{\tilde{t}_1}$. The dashed lines represent the NLO cross section for $\mu = m_{\tilde{t}_1}/2$ and $\mu = 2m_{\tilde{t}_1}$.

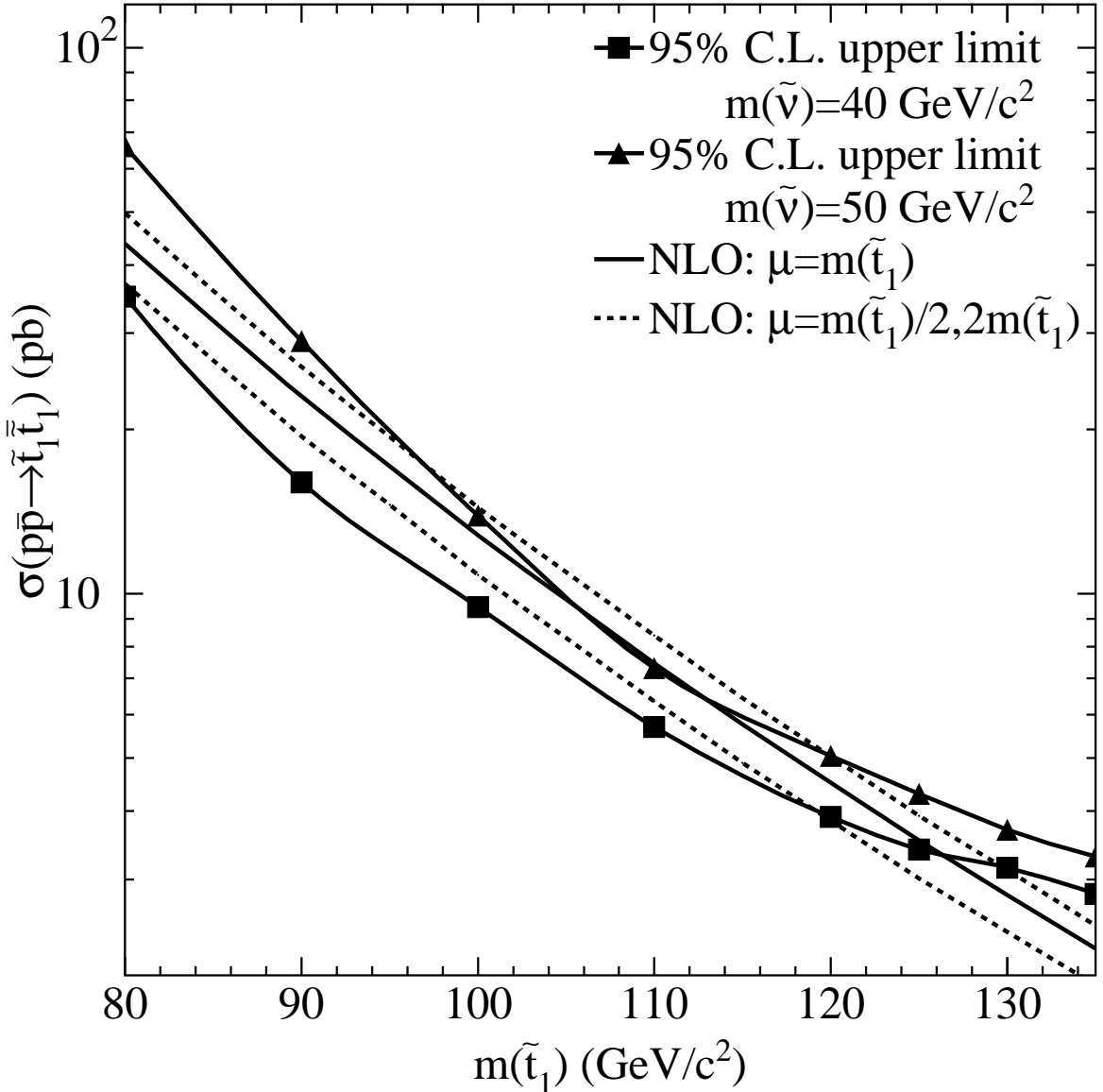


FIG. 3. CDF 95% C.L. cross section limit as a function of \tilde{t}_1 mass when the $\tilde{t}_1 \rightarrow bl^+\tilde{\nu}$ branching ratio is 100% and $m_{\tilde{\nu}} = 40 \text{ GeV}/c^2$ (squares) or $50 \text{ GeV}/c^2$ (triangles). The line without markers represents the NLO prediction for $\sigma_{\tilde{t}_1\bar{t}_1}$ using the renormalization scale $\mu = m_{\tilde{t}_1}$. The dashed lines represent the NLO cross section for $\mu = m_{\tilde{t}_1}/2$ and $\mu = 2m_{\tilde{t}_1}$.

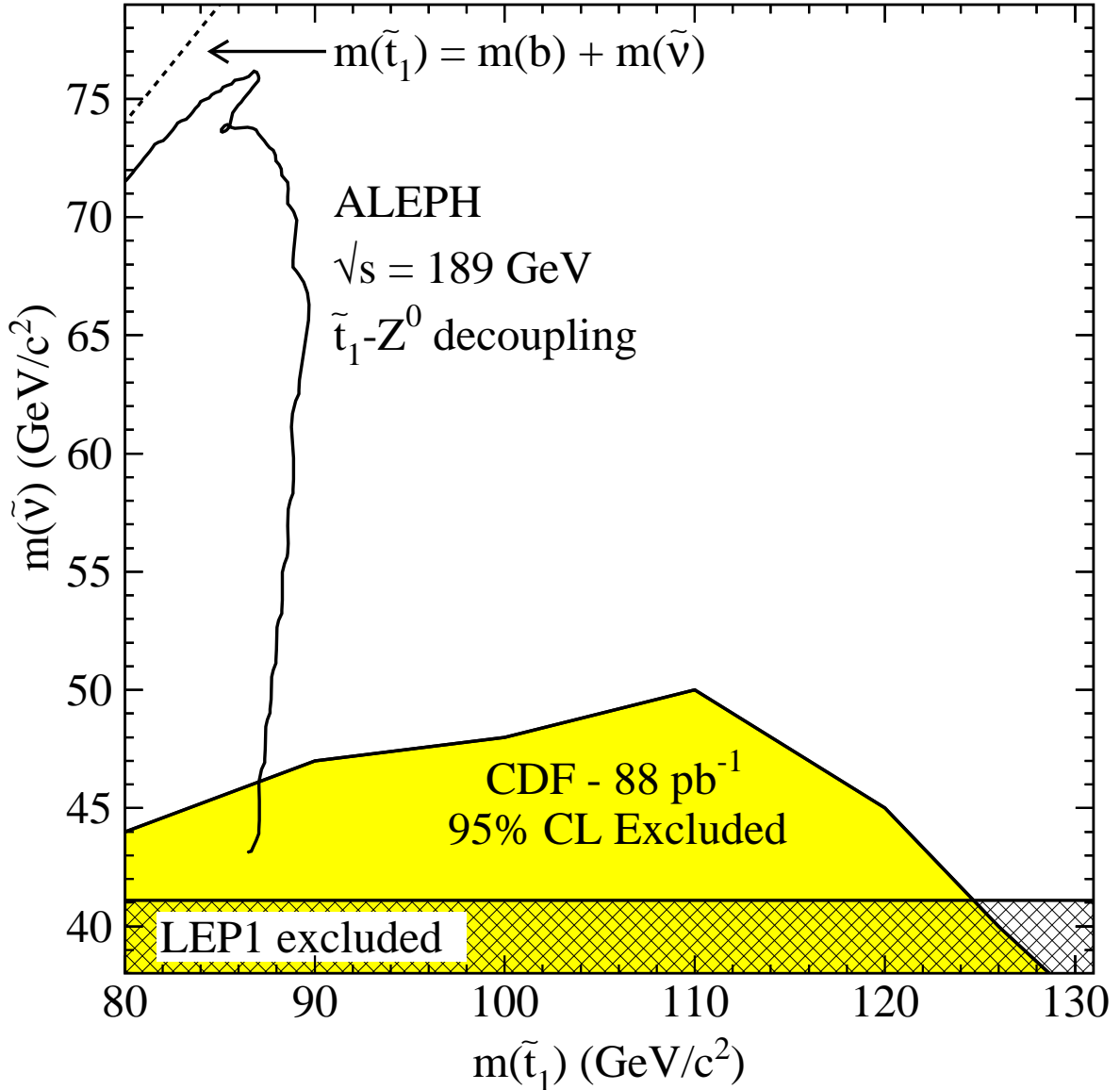


FIG. 4. 95% C.L. excluded region in the plane of $m_{\tilde{t}_1}$ versus $m_{\tilde{\nu}}$ when the $\tilde{t}_1 \rightarrow b e^+ \tilde{\nu}$, $\tilde{t}_1 \rightarrow b \mu^+ \tilde{\nu}$, and $\tilde{t}_1 \rightarrow b \tau^+ \tilde{\nu}$ branching ratios are 33.3%. We define the exclusion region as that region of supersymmetric parameter space for which the 95% C.L. limit on $\sigma_{\tilde{t}_1 \bar{t}_1}$ is less than the NLO prediction ($\mu = m_{\tilde{t}_1}$). The LEP1 $m_{\tilde{\nu}}$ limit and ALEPH excluded region in the $m_{\tilde{t}_1}$ versus $m_{\tilde{\nu}}$ plane are also shown [19]. The ALEPH excluded region corresponds to the case in which the \tilde{t}_1 decouples from the Z^0 .